European Review for Medical and Pharmacological Sciences 2020; 24: 7722-7731

Astaxanthin protecting myocardial cells from hypoxia/reoxygenation injury by regulating miR-138/HIF-1α axis

Y.-S. GAI[1], Y.-H. REN[2], Y. GAO[3], H.-N. LIU[4]

[1]Department of Cardiology, Yantaishan Hospital, Shandong, P.R. China
[2]Department of Cardiology, Liaocheng People's Hospital, Shandong, P.R. China
[3]Department of Cardiology, The People's Hospital of Zhangqiu Area, Jinan, P.R. China
[4]Vasculocardiology Department, Zibo Central Hospital, Shandong, P.R. China

Abstract. – OBJECTIVE: To investigate astaxanthin (AST) protecting myocardial cells from hypoxia/reoxygenation (H/R) injury by regulating miR-138/HIF-1α axis.

MATERIALS AND METHODS: Myocardial cells were collected and divided into a control group, a H/R group, and a H/R+AST group. The H/R injury model was established, and cells in the H/R+AST group were given AST before modeling. The cell survival rate, contents of myocardial enzymes, and apoptosis were detected.

RESULTS: The survival rate in the H/R group reduced and was lower than that in the H/R+AST group ($p<0.05$). Compared with the control group, activities of myocardial enzymes significantly increased in the H/R group but those were inhibited in the H/R+AST group ($p<0.05$). The apoptotic rate in the H/R group significantly increased compared with the control group but that significantly decreased compared with the H/R+AST group ($p<0.05$). The expression of cleaved caspase-9 and caspase-3 increased in the H/R group ($p<0.05$), and was higher than that in the H/R+AST group ($p<0.05$). The expression levels of miR-138 and HIF-1α were detected. MiR-138 level significantly decreased in the H/R group but increased in the H/R+AST group ($p<0.05$). Compared with the control group, HIF-1α content significantly increased in the H/R group but that was significantly inhibited in the H/R+AST group ($p<0.05$). The Luciferase reporter gene assay confirmed that HIF-1α was the target gene of miR-138. After miR-138 mimics and HIF-1α siRNA were transfected into myocardial cells, the cell survival rate significantly increased, and activities of myocardial enzymes were significantly inhibited in the H/R+AST+miR-138 mimics and H/R+AST+HIF-1α siRNA groups ($p<0.05$). The apoptotic rate significantly decreased, and contents of cleaved caspase-9 and caspase-3 were significantly inhibited in the miR-138 mimics and HIF-1α siRNA groups ($p<0.05$).

CONCLUSIONS: AST can exert a protective function in myocardial cells via regulating the expression of miR-138/HIF-1α axis.

Key Words:
AST, MiR-138/HIF-1α axis, Myocardial cells, Protective effect.

Introduction

Acute myocardial infarction is a disease that seriously endangers life and health of patients. Myocardial microcirculation reperfusion, the best method to treat myocardial infarction, reverses myocardial ischemia and limits infarction area[1,2]. However, myocardial reperfusion may cause further tissue injury during treatment, which is often referred to as myocardial reperfusion injury[3]. At present, myocardial ischemia/reperfusion (I/R) injury is a major public health issue worldwide with a high incidence and mortality rate, resulting in approximately 3.4 million female and 3.8 million male deaths every year[4,5]. For better exploring myocardial reperfusion injury, isolated primary myocardial cells with hypoxia/reoxygenation (H/R) are typically used for simulation[6]. As an effective singlet oxygen quencher that has a strong antioxidant effect, astaxanthin (AST) is also a kind of ketone carotene that exists in a variety of organisms many of which are presented in marine environment[7,8]. Literature has shown that AST reduces lipid peroxidation[9], inflammation[10], thrombosis, clearance receptor expression, and activities of macrophage matrix metalloproteinases[11]. Moreover, it inhibits cell apoptosis and improves plaque stability[12], as well as reduces cell

Corresponding Author: Haining Liu, MD; e-mail: dhdsym@sina.cn

fibrosis and improves cardiac function[13]. However, the mechanism of action and pathway of AST remains unclear.

According to previous studies, miRNAs are involved in various biological behaviors of diseases, such as cell apoptosis, proliferation, migration, and cycle procession[14]. Some of them are abnormally expressed during myocardial I/R injury, suggesting that miRNAs may be involved in regulating the progression of the disease[15,16]. It is reported that miR-138 as a miRNA protects myocardial cells from hypoxia-induced injury and is considered as an important regulator in cell signaling pathways[17]. This miR can participate in myocardial cell conduction, anti-ischemic protection, and other links, thus exerting a vital function[18]. It has been confirmed that hypoxia inducible factor-1α (HIF-1α) is abnormally expressed in various human cancers and is an important regulator of steady-state responses to hypoxic cells and systems *in vivo* by activating gene transcription[19,20]. Besides, regulating HIF1-α activity can prevent diabetic cardiomyopathy and cardiac remodeling[21]. MiR-138 can specifically regulate HIF-1α, and the miR-138/HIF-1α axis is involved in the regulation of myocardial ischemia reperfusion injury[22].

In this study, the mechanism of action of AST in the H/R injury of isolated primary myocardial cells was explored, and changes in the miR-138/HIF-1α axis were detected, in order to provide new ideas for treating myocardial ischemia reperfusion.

Materials and Methods

Myocardial Cell Culture and Model Establishment

Myocardial H9C2 cells (YBCC337726) were purchased from ScienCell (Carlsbad, CA, USA). They were placed in a Dulbecco's Modified Eagle's Medium (DMEM) (KL-P0032, Merck/Sigma-Aldrich, Germany) containing 10% fetal bovine serum (FBS), and incubated in an incubator at 37°C and with 5% CO_2. The H/R model was established. After the supernatant in the primarily cultured myocardial cells was discarded, the cell culture fluid was replaced with serum-free DMEM and then cultured in an anoxic box for 12 hours. Next, reoxygenation was performed, and the medium was replaced with DMEM (containing 10% FBS) and then incubated for 4 hours.

Experimental Grouping

Myocardial cells were randomly divided into a normal control group, a H/R group, and a H/R+AST group. The cells in the normal control group cultured at the same time were put into an incubator at 37°C and with 5% CO_2 for the same time. Cells in the H/R group were modeled according to the above method. Cells in the H/R+AST group were treated with 10 μm of AST (SA8730, Solarbio, Beijing, China) before modeling.

Cell Transfection

The cells were transfected and then divided into an empty vector negative control group (H/R+AST+NC), a miR-138 overexpression group (H/R+AST+miR-138 mimics), and a HIF-1α silence group (H/R+AST+HIF-1α siRNA). After the cells adherently grew and fused to 80%-90%, they were respectively transfected according to the instruction of a Lipofectamine™2000 transfection kit (Invitrogen, Carlsbad, CA, USA).

Quantitative-Reverse Transcription-Polymerase Chain Reaction (qRT-PCR)

Total RNA was drawn from the cells using a TRIzol reagent kit (Invitrogen, Carlsbad, CA, USA), and its purity, concentration, and integrity were detected by an UV spectrophotometer and agarose gel electrophoresis. The RNA was reversely transcribed into cDNA according to the instruction of a reverse transcription kit (Thermo Fisher Scientific, Shanghai, China), with the transcribed samples stored at -20°C for later use. A SYBR Premix Ex Taq™ kit (TaKaRa Biotechnology Co, Ltd., Tokyo, Japan) was used for PCR amplification on a PCR instrument (ABI7500, Applied Biosystems, Warrington, UK), with GAPDH and U6 used as internal references. Cycle conditions for the reaction were as follows: denaturation at 95°C for 10 min, denaturation at 95°C for 15 s, and annealing/extension at 60°C for 60 s, for a total of 40 cycles. The data were obtained after three repeated experiments, and the relative expression was calculated by $2^{-\Delta\Delta CT}$ (Table I).

Western Blotting (WB)

Radioimmunoprecipitation assay (RIPA) lysis buffer (Thermo Fisher Scientific, Waltham, MA, USA) was used for lysis, and a bicinchoninic acid (BCA) protein assay kit (Thermo Fisher Scientific, Waltham, MA, USA) was used to detect the protein concentration. After the concentration was adjusted to 4 μg/μL, the protein was separated by 12% sodium dodecyl sulfate polyacryl-

Table I. Primer sequences.

	Forward	Reverse
miR-138	5′-AGCTGGTGTTGTGAATC-3′	5′-GTGCAGGGTCCGAGGT-3′
U6	5’-CGGGTTTGTTTTGCATTTGT-3’	5’-AGTCCCAGCATGAACAGCTT-3’
HIF-1α	5’-CACCACAGGACAGTACAGGAT-3’	5’-CGTGCTGAATAATACCACTCACA-3’
GAPDH	5’-CTGGGCTACACTGAGCACC-3’	5’-AAGTGGTCGTTGAGGGCAATG-3’

amide gel electrophoresis (SDS-PAGE), transferred to polyvinylidene difluoride (PVDF) membrane (Millipore, Billerica, MA, USA), and then sealed in 5% skimmed milk for immune reaction. Next, the membrane was incubated with primary antibody (Santa Cruz Biotechnology, Santa Cruz, CA, USA) (1:1000) overnight at 4°C. After washed to remove the primary antibody, the membrane was added with horseradish peroxidase-labeled goat anti-rabbit secondary antibody (Abcam, Cambridge, MA, USA) (1:1000), incubated at 37°C for 1 hour, and rinsed with phosphate-buffered saline (PBS) over 5 min for 3 times. After that, the membrane was developed with an enhanced chemiluminescence (ECL) reagent (Thermo Fisher Scientific, Waltham, MA, USA) and then fixed. The Quantity One infrared imaging system was used for photographing. The relative expression level of the protein = the gray value of the band /the gray value of the internal reference.

Detection of Cell Survival Rate

Cell counting kit-8 (CCK-8; Nanjing Enogene Biotech Co., Ltd., China) was used to analyze the cell survival rate. The isolated and extracted primary myocardial cells were inoculated into a 96-well plate (6×10^3 cells/well), and then added again with 200 μL of medium (containing 20 μL of CCK-8) for continuous incubation for 4 hours. The optical density (OD) value of each group was detected at 450 nm using the Multiskan FC microplate reader (Thermo Fisher Scientific, Waltham, MA, USA).

Detection of Apoptosis

Annexin V-FITC/Propidium Iodide (PI) apoptosis detection kit (Becon Dickinson FACSCalibur, CA, USA) was used for detection. Cells were digested with trypsin, washed with PBS for twice, and then collected into centrifuge tubes. Next, 20 μL of labeled Annexin-V-FITC solution was first added to 1 mL of buffer solution, and 20 μL of PI reagent was then added. Cells were finally incubated at room temperature in the dark for 5 min. The Beckman Coulter CytoFLEX LX flow cytometer system was used for detection. The experiment was repeatedly carried out for 3 times to obtain the average value.

Determination of Lactate Dehydrogenase (LDH), Cardiac Troponin I (cTnI), and Creatine Kinase-MB (CK-MB)

After H/R injury, cell supernatants of each group were collected. Enzyme-linked immunosorbent assay (ELISA) was used to detect contents of LDH (RL008, Shanghai Gefan Biotechnology Co., Ltd., China), CK-MB (RC044, Shanghai Gefan Biotechnology Co., Ltd., China), and cTnI (EKC40439, R&D Systems Inc., China), with operating steps strictly carried out in accordance with the kit instruction. The OD value was detected using the Multiskan FC microplate reader at 450 nm.

Luciferase Reporter Gene Assay

TargetScan was used to predict the binding site of miR-138 and HIF-1α. Subsequently, a fragment of HIF-1α 3’-untranslated region (3’-UTR; containing the wild type (HIF-1α wt) or mutation (HIF-1α mut) of the predicted binding site) was cloned on the vector. After verification with DNA sequencing, the plasmids (miR-138 mimics, NC mimics) were transfected into myocardial cells according to the instruction of a Lipofectamine™2000 kit (Invitrogen, Carlsbad, CA, USA). The cells were collected at 48 hours after transfection. The Dual-Luciferase reporter gene assay system (DLR® Promega Corporation, Madison, WI, USA) was used for analysis.

Statistical Analysis

SPSS 20.0 software package (IBM, Armonk, NY, USA) was used to statistically analyze the collected data. GraphPad 7 software package (La Jolla, CA, USA) was used to plot the required figures. The comparison between two groups was analyzed by *t*-test, and the comparison between multiple groups was analyzed by one-way ANOVA, and LSD-t test was used for post-hoc pair-

wise comparison. $p<0.05$ indicated a statistically significant difference.

Results

Effects of AST on H/R-Induced Myocardial Cell Injury (MCI)

As shown in Figure 1, the survival rate of myocardial cells in the H/R group decreased significantly, and was lower than that in the H/R+AST group ($p<0.05$). Compared with the control group, activities of LDH, CK-MB, and cTnI significantly increased in the H/R group ($p<0.05$), but those were significantly inhibited in the H/R+AST group ($p<0.05$).

Effects of AST on H/R-Induced Myocardial Cell Apoptosis

Cell apoptosis in each group is shown in Figure 2. The apoptotic rate significantly increased in the H/R group compared with the other two groups ($p<0.05$), and the rate in the H/R+AST group was significantly lower than that in the H/R group but higher than that in the control group ($p<0.05$). The expression of cleaved caspase-9 and caspase-3 in each group was detected. Their expression and contents significantly increased in the H/R group compared with the other two groups ($p<0.05$), and the expression and contents significantly increased in the H/R+AST group compared with the control group ($p<0.05$).

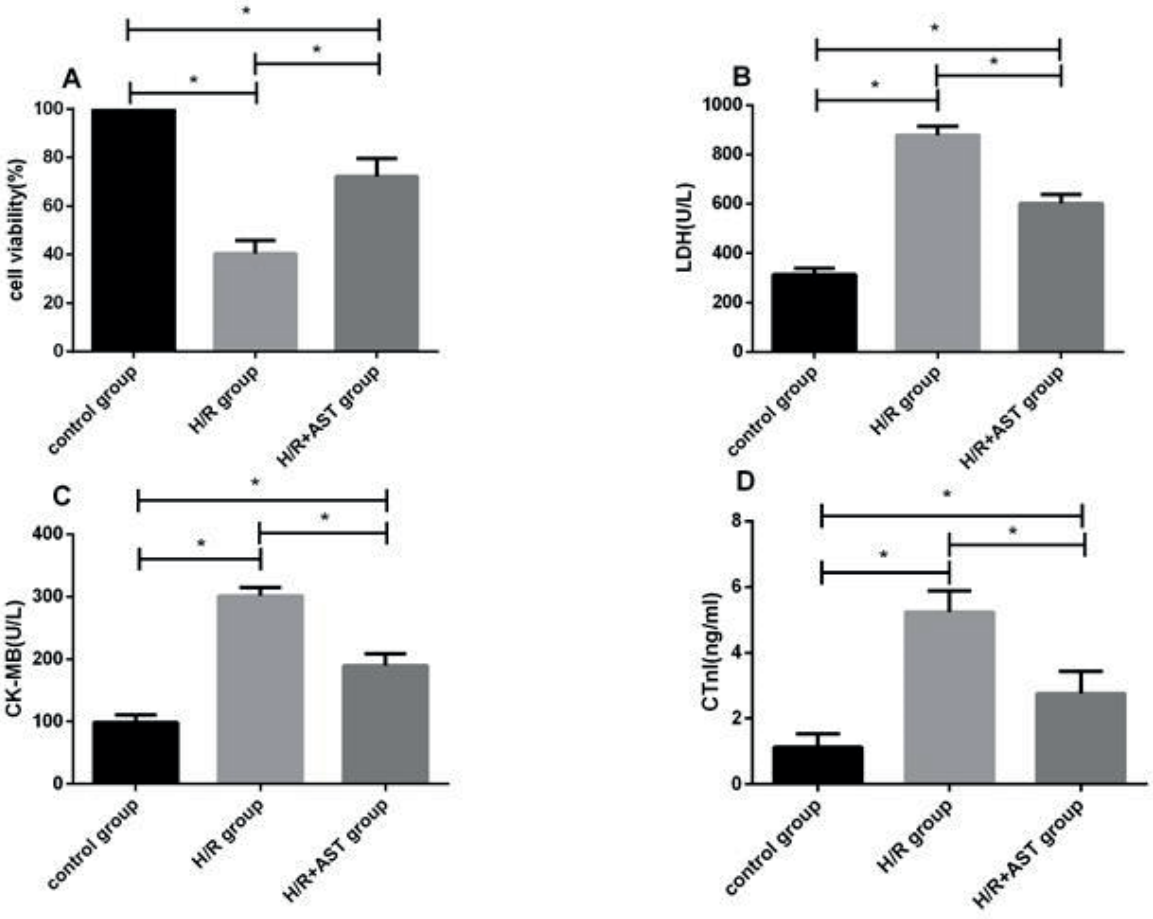

Figure 1. Effects of AST on H/R-induced MCI. **A,** The comparison of cell survival rate. **B,** The comparison of LDH activity. **C,** The comparison of CK-MB activity. **D,** The comparison of cTnI activity. Note: * indicates a comparison between two groups, $p<0.05$.

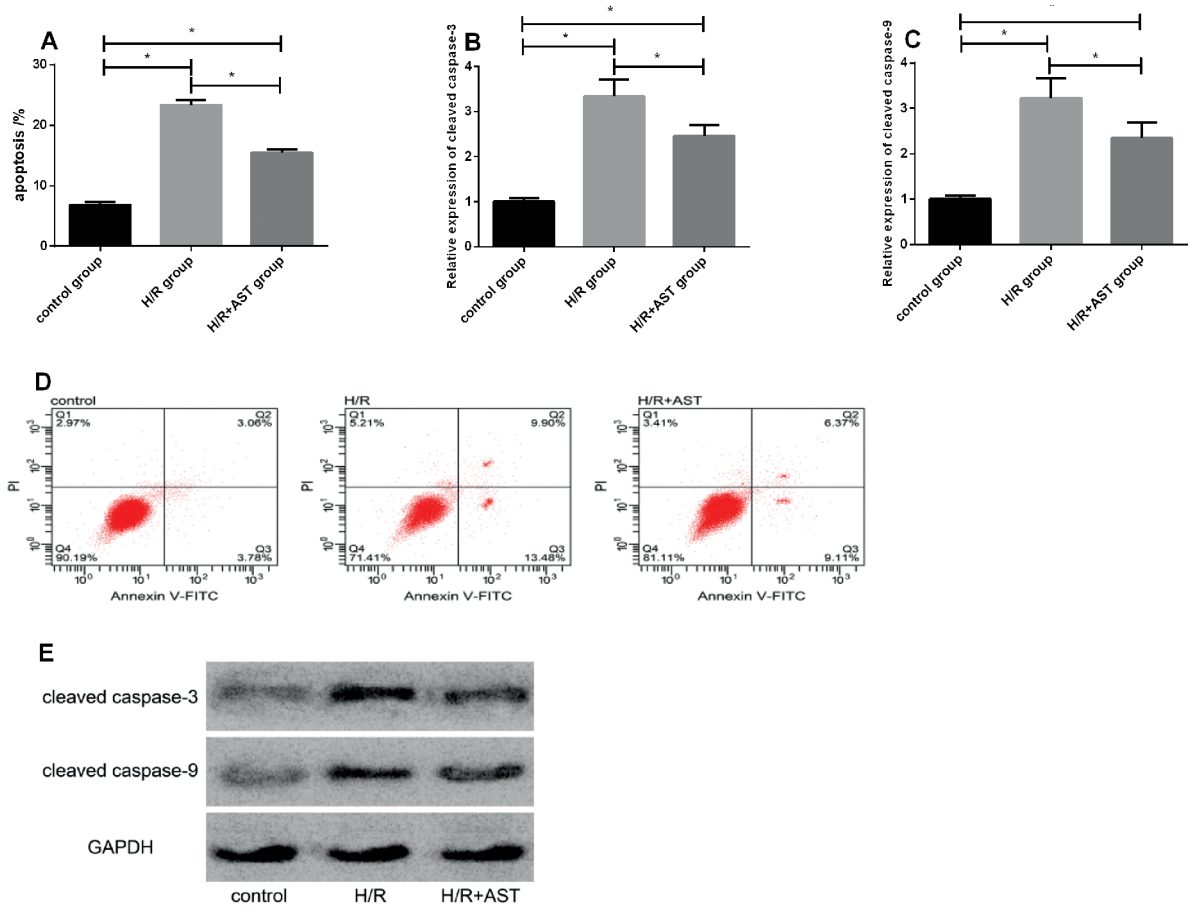

Figure 2. Effects of AST on H/R-induced myocardial cell apoptosis. **A,** The comparison of cell apoptotic rate. **B,** The comparison of caspase-3 expression. **C,** The comparison of caspase-9 expression. **D,** A myocardial cell apoptosis map. **E,** A map for caspase-3 and caspase-9 proteins. Note: * indicates a comparison between two groups, p<0.05.

Effects of AST on MiR-138 and HIF-1α Levels

The expression levels of miR-138 and HIF-1α in the control, H/R, and H/R+AST groups were detected, respectively, as shown in Figure 3. MiR-138 level in the H/R group decreased significantly compared with the control group, but increased compared with the H/R+AST group (p<0.05). Compared with the control group, the mRNA level and protein content of HIF-1α significantly increased in the H/R group, while those significantly decreased in the H/R+AST group (p<0.05).

Verification of the Relationship Between MiR-138 and HIF-1α

Bioinformatics results were confirmed by the Luciferase reporter gene assay. As shown in Figure 4, HIF-1α was found to be the target gene of miR-138. After the transfection of miR-138 mimics, the Luciferase activity of HIF-1α-Wt was significantly inhibited (p<0.05). The expression and content of HIF-1α in the miR-138 mimics group were significantly lower than those in the NC group (p<0.05).

AST Exerting Myocardial Protection Through MiR-138/HIF-1α Axis

The corresponding miR-138 mimics and HIF-1α siRNA were transfected into myocardial cells. As shown in Figure 5, the cell survival rate increased significantly, and activities of LDH, CK-MB, and cTnI were significantly inhibited in the H/R+AST+miR-138 mimics and H/R+AST+HIF-1α siRNA groups (p<0.05). The apoptotic rate decreased significantly (p<0.05), and contents of cleaved caspase-9 and caspase-3 were significantly inhibited in the miR-138 mimics and HIF-1α siRNA groups (p<0.05).

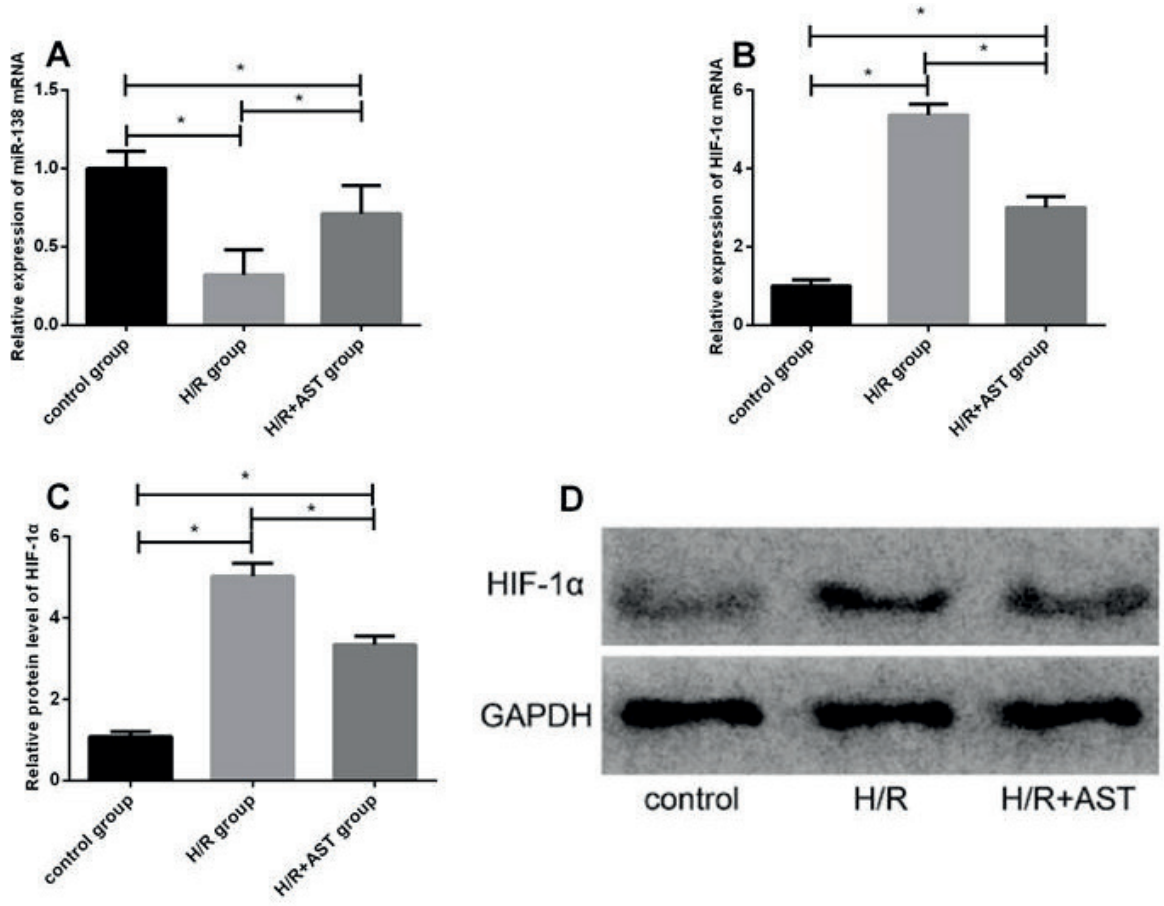

Figure 3. Effects of AST on miR-138 and HIF-1α levels. **A,** Effects of AST on miR-138 level. **B,** Effects of AST on HIF-1α level. **C,** Effects of AST on the OD of HIF-1α. **D,** Effects of AST on HIF-1α expression. Note: * indicates a comparison between two groups, $p<0.05$.

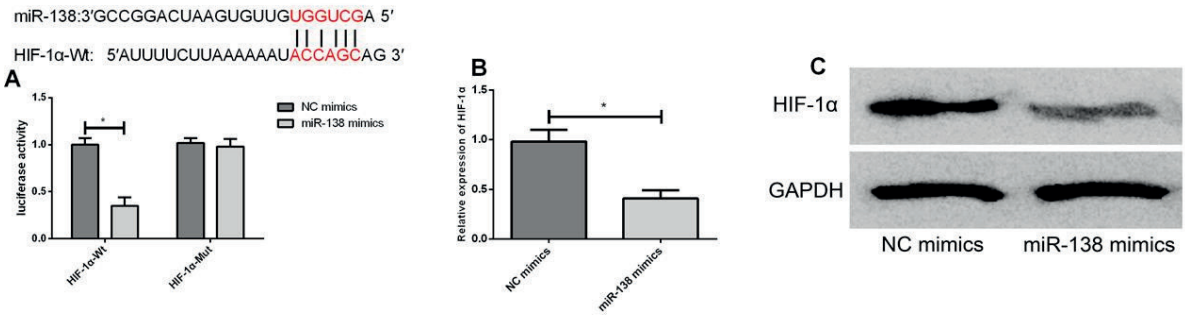

Figure 4. Validation of the relationship between miR-138 and HIF-1α. **A,** The verification of HIF-1α being the target gene of miR-138. **B,** Changes in HIF-1α expression after transfection. **C,** Changes in HIF-1α content after transfection. Note: * indicates a comparison between the two groups, $p<0.05$.

Discussion

Mainly occurring in the process of myocardial infarction, H/R not only leads to myocardial microvascular damage, but also damages great vessels[23]. Additionally, it damages various physiological activities of endothelial cells, such as cell survival rate reduction, energy metabolism disorder, angiogenesis damage, the excess production of reactive oxygen species, and mitochondrial

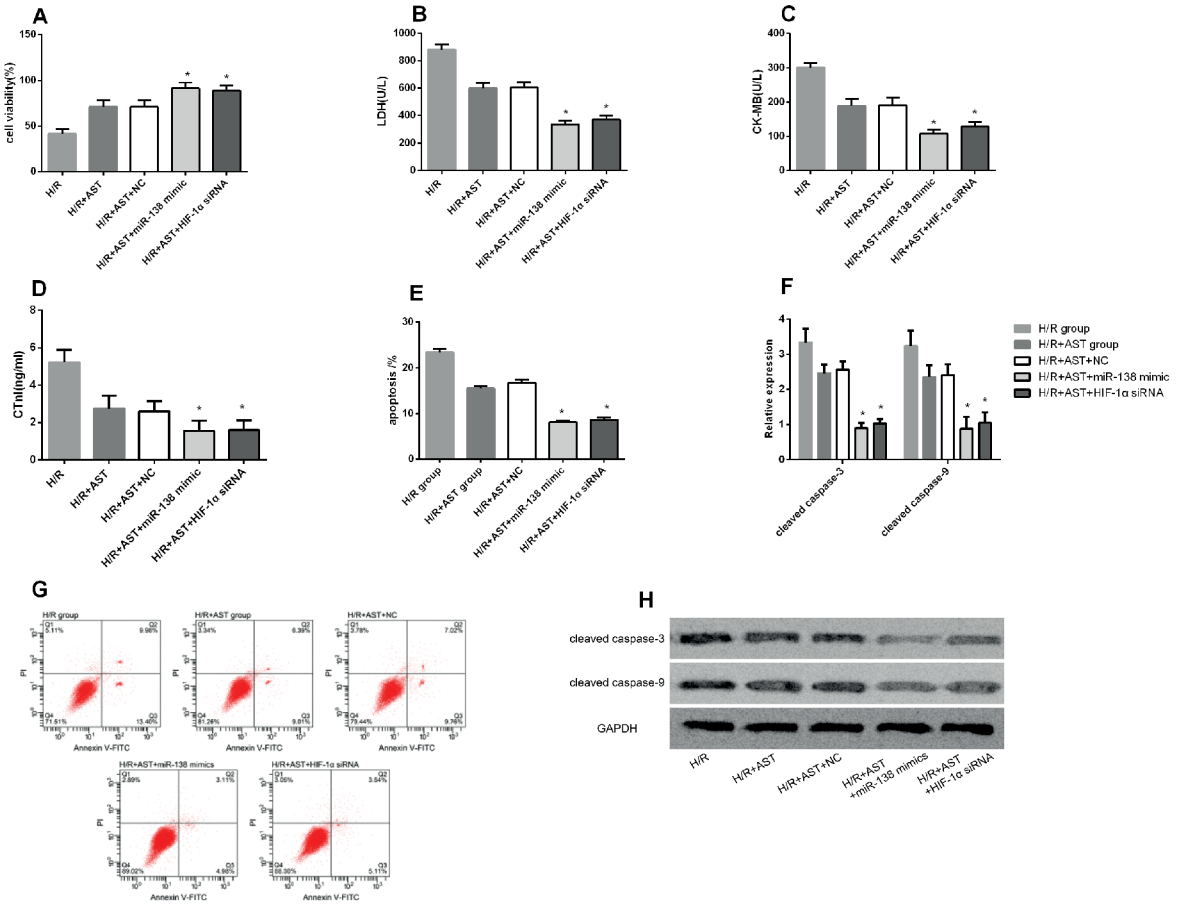

Figure 5. AST exerting myocardial protection through miR-138/HIF-1α axis. **A,** The comparison of cell survival rate after transfection. **B,** LDH changes after transfection. **C,** The comparison of CK-MB after transfection. **D,** The comparison of cTnI expression after transfection. **E,** The comparison of apoptotic rate after transfection. **F,** The comparison of caspase-9 and caspase-3 contents after transfection. **G,** An apoptosis map after transfection. **H,** A map for caspase-9 and caspase-3 proteins. Note: * indicates $p<0.05$ compared with the H/R, H/R+AST, and H/R+AST+NC groups.

dysfunction[24]. AST is a symmetrical molecule composed of two terminal rings that are connected by a short polyene ring. Natural AST mainly exists in an esterified form, while synthetic AST is produced in a free form[25]. AST protects heart by improving body inflammation, oxidative stress, lipid metabolism, and glucose metabolism[26], but its specific mechanism of action in H/R is still unclear.

LDH is a biochemical index and changes in its activity reflect the degree of MCI, so this index can be used to assess myocardial injury with good repeatability and high reliability[27]. Presented in myocardial cells and involved in the regulation of substance metabolism and cell energy, CK-MB and cTnI can be also used to detect MCI[28]. When cells are cultured *in vitro*, H/R-induced MCI causes cell rupture and the release of metabolic enzymes in cytoplasm outside cells[29]. Studies[22,30,31] have found that H/R occurrence increases activities of LDH, CK-MB, and cTnI and the apoptotic rate of myocardial cells. In our study, H/R-induced MCI decreased the cell survival rate and increased activities of the three enzymes, which indicates that H/R causes myocardial cell rupture and metabolic enzyme release into the culture medium. AST can relieve MCI and reduce contents of metabolic enzymes entering the culture medium. According to He et al[32], esculetin can inhibit the oxidative stress and apoptosis of H/R myocardial H9c2 cells; AST can inhibit neuronal apoptosis in insulin-resistant mice[33]. Caspase-9 and caspase-3 are both involved in the development and progression of cell apoptosis. As the key protease of mitochondrial apoptosis pathways, the former causes cascade reaction through self-splic-

ing activation, thus activating apoptosis executors such as the latter[34,35]. H/R injury is closely related to mitochondrial apoptosis[36]. In our study, AST could inhibit the apoptosis of H/R-induced myocardial cells as well as the expression of cleaved caspase-9 and caspase-3, thereby inhibiting the apoptosis of mitochondrial pathways.

MiR-138 is lowly expressed but HIF-1α is highly expressed in H/R-induced myocardial cells[22]. Zhang et al[37] have found that emodin protects H9c2 cells from hypoxia-induced damage through up-regulating miR-138 expression, while silencing the expression weakens the protection. In our study, the expression levels of miR-138 and HIF-1α in different groups were detected, respectively. MiR-138 level significantly decreased and HIF-1α content significantly increased in the H/R group, while the decrease and the increase were reversed after treatment with AST. This shows that AST can regulate miR-138 and HIF-1α. The relationship between miR-138 and HIF-1α was confirmed by the Luciferase reporter gene assay. HIF-1α was the target gene of miR-138, and the Luciferase activity of HIF-1α-Wt was significantly inhibited in the miR-138 mimics group. The expression and content of HIF-1α in the miR-138 mimics group were significantly lower than those in the NC group ($p<0.05$). These results have been confirmed in previous studies[22,38]. Liu et al[39] put forward that AST can alleviate acute renal injury induced *in vivo* and *vitro* by regulating the expression of SIRT1/FOXO3a axis. It also plays a protective role by inhibiting NF-κB/MAPKs signaling pathway in inflammatory responses induced by Ophiocephalus argus lipopolysaccharide[40]. To further explore the mechanism of action of AST on myocardial cells with H/R injury, we transfected miR-138 mimics and HIF-1α siRNA into the cells. Their survival rate significantly increased, and activities of LDH, CK-MB, and CTnI were significantly inhibited in the H/R+AST+miR-138 mimics and H/R+AST+HIF-1α siRNA groups. The apoptotic rate decreased significantly, and contents of cleaved caspase-9 and caspase-3 were significantly inhibited in the miR-138 mimics and HIF-1α siRNA groups ($p<0.05$). These findings demonstrate that AST may regulate biological behaviors of myocardial cells by regulating the miR-138/HIF-1α axis, thus playing a protective role.

Conclusions

We mainly explored the mechanism of action of AST in H/R-induced myocardial injury, and found that AST could exert a protective function via regulating the miR-138/HIF-1α axis, which provides some ideas for future research and treatment. However, there are certain limitations to this study. Due to many regulatory pathways for myocardial injury, whether there are other pathways remains to be further studied and verified. Moreover, whether AST can participate in cellular inflammatory and oxidative stress responses through the regulation of miR-138/HIF-1α still needs more basic research to confirm. In summary, AST affects biological behaviors of myocardial cells via regulating the miR-138/HIF-1α axis, thereby exerting a protective function.

Conflict of Interest

The Authors declare that they have no conflict of interests.

References

1) Otterspoor LC, van Nunen LX, van 't Veer M, Johnson NP, Pijls NHJ. Intracoronary hypothermia before reperfusion to reduce reperfusion injury in acute myocardial infarction: a novel hypothesis and technique. Ther Hypothermia Temp Manag 2017; 7: 199-205.
2) Fordyce CB, Gersh BJ, Stone GW, Granger CB. Novel therapeutics in myocardial infarction: targeting microvascular dysfunction and reperfusion injury. Trends Pharmacol Sci 2015; 36: 605-616.
3) Takatori O, Usui S, Okajima M, Kaneko S, Ootsuji H, Takashima SI, Kobayashi D, Murai H, Furusho H, Takamura M. Sodium 4-phenylbutyrate attenuates myocardial reperfusion injury by reducing the unfolded protein response. J Cardiovasc Pharmacol Ther 2017; 22: 283-292.
4) Sun MY, Ma DS, Zhao S, Wang L, Ma CY, Bai Y. Salidroside mitigates hypoxia/reoxygenation injury by alleviating endoplasmic reticulum stress-induced apoptosis in H9c2 myocardial cells. Mol Med Rep 2018; 18: 3760-3768.
5) Yellon DM, Hausenloy DJ. Myocardial reperfusion injury. N Engl J Med 2007; 357: 1121-1135.
6) Portal L, Martin V, Assaly R, d'Anglemont de Tassigny A, Michineau S, Berdeaux A, Ghaleb B, Pons S. A model of hypoxia-reoxygenation on isolated adult mouse myocardial cells: characterization, comparison with ischemia-reperfusion, and application to the cardioprotective effect of regular treadmill exercise. J Cardiovasc Pharmacol Ther 2013; 18: 367-375.
7) Balci Yuce H, Lektemur Alpan A, Gevrek F, Toker H. Investigation of the effect of astaxanthin on alveolar bone loss in experimental periodontitis. J Periodontal Res 2018; 53: 131-138.
8) Fassett R G, Coombes J S. Astaxanthin in cardiovascular health and disease. Molecules 2012; 17: 2030-2048.

9) Xu J, Rong S, Gao H, Chen C, Yang W, Deng Q, Huang Q, Xiao L, Huang F. A combination of flaxseed oil and astaxanthin improves hepatic lipid accumulation and reduces oxidative stress in high fat-diet fed rats. Nutrients 2017; 9: 271.

10) Park JS, Chyun JH, Kim YK, Line LL, Chew BP. Astaxanthin decreased oxidative stress and inflammation and enhanced immune response in humans. Nutr Metab (Lond) 2010; 7: 18.

11) Kishimoto Y, Tani M, Uto-Kondo H, Iizuka M, Saita E, Sone H, Kurata H, Kondo K. Astaxanthin suppresses scavenger receptor expression and matrix metalloproteinase activity in macrophages. Eur J Nutr 2010; 49: 119-126.

12) Li W, Hellsten A, Jacobsson LS, Blomqvist HM, Olsson AG, Yuan XM. Alpha-tocopherol and astaxanthin decrease macrophage infiltration, apoptosis and vulnerability in atheroma of hyperlipidaemic rabbits. J Mol Cell Cardiol 2004; 37: 969-978.

13) Zhang J, Wang QZ, Zhao SH, Ji X, Qiu J, Wang J, Zhou Y, Cai Q, Zhang J, Gao HQ. Astaxanthin attenuated pressure overload-induced cardiac dysfunction and myocardial fibrosis: partially by activating SIRT1. Biochim Biophys Acta Gen Subj 2017; 1861: 1715-1728.

14) Pishkari S, Paryan M, Hashemi M, Baldini E, Mohammadi-Yeganeh S. The role of microRNAs in different types of thyroid carcinoma: a comprehensive analysis to find new miRNA supplementary therapies. J Endocrinol Invest 2018; 41: 269-283.

15) Guedes EC, da Silva IB, Lima VM, et al. High fat diet reduces the expression of miRNA-29b in heart and increases susceptibility of myocardium to ischemia/reperfusion injury. J Cell Physiol 2019; 234: 9399-9407.

16) Lorenzen JM, Batkai S, Thum T. Regulation of cardiac and renal ischemia-reperfusion injury by microRNAs. Free Radic Biol Med 2013; 64: 78-84.

17) Xiong H, Luo T, He W, Xi D, Lu H, Li M, Liu J, Guo Z. Up-regulation of miR-138 inhibits hypoxia-induced cardiomyocyte apoptosis via down-regulating lipocalin-2 expression. Exp Biol Med 2016; 241: 25-30.

18) Salloum FN, Yin C, Kukreja RC. Role of microRNAs in cardiac preconditioning. J Cardiovasc Pharmacol 2010; 56: 581-588.

19) Masoud GN, Li W. HIF-1α pathway: Role, regulation and intervention for cancer therapy. Acta Pharm Sin B 2015; 5: 378-389.

20) Williams AL, Walton CB, MacCannell KA, Avelar A, Shohet RV. HIF-1 regulation of miR-29c impairs SERCA2 expression and cardiac contractility. Am J Physiol Heart Circ Physiol 2019; 316: H554-H565.

21) Xue W, Cai L, Tan Y, Thistlethwaite P, Kang YJ, Li X, Feng W. Cardiac-specific overexpression of HIF-1{alpha} prevents deterioration of glycolytic pathway and cardiac remodeling in streptozotocin-induced diabetic mice. Am J Pathol 2010; 177: 97-105.

22) Liu Y, Zou J, Liu X, Zhang Q. MicroRNA-138 attenuates myocardial ischemia reperfusion injury through inhibiting mitochondria-mediated apoptosis by targeting HIF1-α. Exp Ther Med 2019; 18: 3325-3332.

23) Hausenloy DJ, Yellon DM. Ischemic conditioning and reperfusion injury. Nat Rev Cardiol 2016; 13: 193-209.

24) Wang Y, Han X, Fu M, Wang J, Song Y, Liu Y, Zhang J, Zhou J, Ge J. Qiliqiangxin attenuates hypoxia-induced injury in primary rat cardiac microvascular endothelial cells via promoting HIF-1α-dependent glycolysis. J Cell Mol Med 2018; 22: 2791-2803.

25) Wu H, Niu H, Shao A, Wu C, Dixon BJ, Zhang J, Yang S, Wang Y. Astaxanthin as a potential neuroprotective agent for neurological diseases. Mar Drugs 2015; 13: 5750-5766.

26) Kishimoto Y, Yoshida H, Kondo K. Potential anti-atherosclerotic properties of astaxanthin. Mar Drugs 2016; 14: 35.

27) Ghiasi R, Mohammadi M, Majidinia M, Yousefi B, Ghiasi A, Badalzadeh R. The effects of mebudipine on myocardial arrhythmia induced by ischemia-reperfusion injury in isolated rat heart. Cell Mol Biol (Noisy-le-grand) 2016; 62: 15-20.

28) Liang D, Zhong P, Hu J, Lin F, Qian Y, Xu Z, Wang J, Zeng C, Li X, Liang G. EGFR inhibition protects cardiac damage and remodeling through attenuating oxidative stress in STZ-induced diabetic mouse model. J Mol Cell Cardiol 2015; 82: 63-74.

29) Kalogeris T, Baines C P, Krenz M, Korthuis RJ. Cell biology of ischemia/reperfusion injury[M]//Int Rev Cell Mol Biol. Academic Press 2012; 298: 229-317.

30) Wang W, Huang X, Shen D, Ming Z, Zheng M, Zhang J. Polyphenol epigallocatechin-3-gallate inhibits hypoxia/reoxygenation-induced H9C2 cell apoptosis. Minerva Med 2018; 109: 95-102.

31) Chen J, Jiang Z, Zhou X, Sun X, Cao J, Liu Y, Wang X. Dexmedetomidine preconditioning protects myocardial cells against hypoxia/reoxygenation-induced necroptosis by inhibiting HMGB1-mediated inflammation. Cardiovasc Drugs Ther 2019; 33: 45-54.

32) He Y, Li C, Ma Q, Chen S. Esculetin inhibits oxidative stress and apoptosis in H9c2 myocardial cells following hypoxia/reoxygenation injury. Biochem Biophys Res Commun 2018; 501: 139-144.

33) Galasso C, Orefice I, Pellone P, Cirino P, Miele R, Ianora A, Brunet C, Sansone C. On the neuroprotective role of astaxanthin: new perspectives? Mar Drugs 2018; 16: 247.

34) Mitupatum T, Aree K, Kittisenachai S, Roytrakul S, Puthong S, Kangsadalampai S, Rojpibulstit P. mRNA Expression of Bax, Bcl-2, p53, Cathepsin B, Caspase-3 and Caspase-9 in the HepG2 cell line following induction by a novel monoclonal Ab Hep88 mAb: cross-talk for paraptosis and apoptosis. Asian Pac J Cancer Prev 2016; 17: 703-712.

35) Zhao W, Yang Y, Zhang Y X, Zhou C, Li HM, Tang YL, Liang XH, Chen T, Tang YJ. Fluoride-containing podophyllum derivatives exhibit antitumor

activities through enhancing mitochondrial apoptosis pathway by increasing the expression of caspase-9 in HeLa cells. Sci Rep 2015; 5: 17175.

36) Maruyama D, Hirata N, Miyashita R, Kawaguchi R, Yamakage M. Substrate-dependent modulation of oxidative phosphorylation in isolated mitochondria following in vitro hypoxia and reoxygenation injury. Exp Clin Cardiol 2013; 18: 158-160.

37) Zhang X, Qin Q, Dai H, Cai S, Zhou C, Guan J. Emodin protects H9c2 cells from hypoxia-induced injury by up-regulating miR-138 expression. Braz J Med Biol Res 2019; 52: e7994.

38) Sen A, Most P, Peppel K. Induction of microRNA-138 by pro-inflammatory cytokines causes endothelial cell dysfunction. FEBS Lett 2014; 588: 906-914.

39) Liu N, Chen J, Gao D, Li W, Zheng D. Astaxanthin attenuates contrast agent-induced acute kidney injury in vitro and in vivo via the regulation of SIRT1/FOXO3a expression. Int Urol Nephrol 2018; 50: 1171-1180.

40) Li M Y, Sun L, Niu X T, Chen XM, Tian JX, Kong YD, Wang GQ. Astaxanthin protects lipopolysaccharide-induced inflammatory response in Channa argus through inhibiting NF-κB and MAPKs signaling pathways. Fish Shellfish Immunol 2019; 86: 280-286.